In Situ Raman Microscopy of a Single Graphite Microflake Electrode in a Li^+-Containing Electrolyte

Qingfang Shi, Kaoru Dokko, and Daniel A. Scherson*

Department of Chemistry, Case Western Reserve University, Cleveland, Ohio 44106-7078

Received: October 7, 2003; In Final Form: February 9, 2004

Highly detailed Raman spectra from a single KS-44 graphite microflake electrode as a function of the applied potential have been collected in situ using a Raman microscope and a sealed spectroelectrochemical cell isolated from the laboratory environment. Correlations were found between the Raman spectral features and the various Li^+ intercalation stages while recording in *real time* Raman spectra during a linear potential scan from 0.7 V down ca. 0.0 V vs Li/Li^+ at a rate of 0.1 mV/s in a 1 M $LiClO_4$ solution in a 1:1 (by volume) ethylene carbonate (EC):diethyl carbonate (DEC) mixture. In particular, clearly defined isosbestic points were observed for data collected in the potential range where the transition between dilute phase 1 and phase 4 of lithiated graphite is known to occur, i.e., $0.174 \leq E \leq 0.215$ V vs Li/Li^+. Statistical analysis of the spectroscopic data within this region made it possible to determine *independently* the fraction of each of the two phases present as a function of potential without relying on coulometric information and then predict, on the basis of proposed stoichiometry for the transition, a *spectrally derived* voltammetric feature.

Introduction

Continuing progress is being made in our laboratories toward developing Raman microscopy as a time- and space-resolved probe of electrodes within actual battery environments.[1,2] Much of the impetus for research in this area stems from the possibility of visualizing charge flow within energy storage devices during operation, which may serve to validate and/or refine theoretical models aimed at predicting from first principles their electrical response. Raman scattering affords a convenient means of monitoring the incorporation and release of Li^+ from a variety of host lattices, including transition metal oxides[3−10] and graphite,[11−14] as, in most instances, changes in the molar fraction of Li^+ elicit corresponding modifications in the spectral properties of the materials. Useful information has been gained from spectroelectrochemical experiments under steady-state conditions, allowing direct correlations to be made between spectra and state of charge of (or equivalently extent of Li^+ intercalation within) specimens containing the same constituents as those found in practical electrodes.[1,12−14] More recently, interfering effects due to binders and additives have been eliminated by embedding ensembles of individual particles into judiciously selected substrates.[11,12,15] In fact, the use of a Raman microscope attachment has made it possible to focus the exciting laser radiation onto individual particles in such ensembles, enabling certain aspects of the dynamics of Li^+ intercalation within such single particles to be monitored in real time.[12] One of the disadvantages of this latter strategy is that the electrochemical response represents a convolution of all particles within the ensemble, making it difficult to correlate the recorded spectra with the observed current. An approach that can overcome part of these difficulties, developed by Uchida and co-workers, combines micromanipulation techniques with microelectrodes to perform electrochemical experiments on single microparticle electrodes.[16−19] In fact, implementation of some of those methodologies in our laboratory culminated recently in the first in situ Raman spectroelectrochemical experiments of single particle Li^+ intercalation electrodes using a lithiated Mn oxide as a model system.[20] The extraordinary high quality of the spectra acquired in that study provided clear evidence that in the range $15 < \mathrm{SOD} < 45\%$, where SOD represents the state of discharge (in percent) of the nominally fully charged material, i.e., λ-MnO_2, two distinct phases of lithiated metal oxide coexist, in agreement with information derived from in situ X-ray diffraction (XRD) measurements involving more conventional battery-type electrodes. This contribution extends the procedures therein described to a single KS-44 graphite microflake using a spectroelectrochemical cell specifically designed to isolate the cell components and electrolyte from the laboratory environment. As will be shown, highly detailed voltammetric and Raman scattering information recorded *simultaneously* were found to be in excellent agreement with data reported in the literature for both techniques applied independently.

Experimental Section

The spectroelectrochemical cell used in these measurements was the same as that described earlier for experiments involving lithiated Mn oxide in nonaqueous electrolytes. To avoid problems with Li alloy formation, a Ni (instead of a Au) microelectrode was used as the current collector. This Ni microelectrode was fabricated by inserting a thin Ni wire (50 μm in diameter) into a glass tube and heating the tip of the tube in a hydrogen flame above the melting point to totally encapsulate the Ni wire. Once allowed to cool to room temperature, the tip was polished with sandpaper (CARBIMET, Grit600) to expose a flat, circularly shaped surface. Once installed in the cell, the Ni microelectrode was turned upward (surface facing up) under a regular microscope, and a single KS-44 microflake placed in its center. Immediately thereafter, the sapphire window (Esco Products Inc., 0.5 mm thick) was positioned above the flake/electrode and pressed downward against the cell body via an O-ring (KALREZ) using a clamp to trap firmly the flake between the window and the Ni current collector. This assembly was then transferred to a high-quality

10.1021/jp037015e CCC: $27.50
Published on Web 03/20/2004

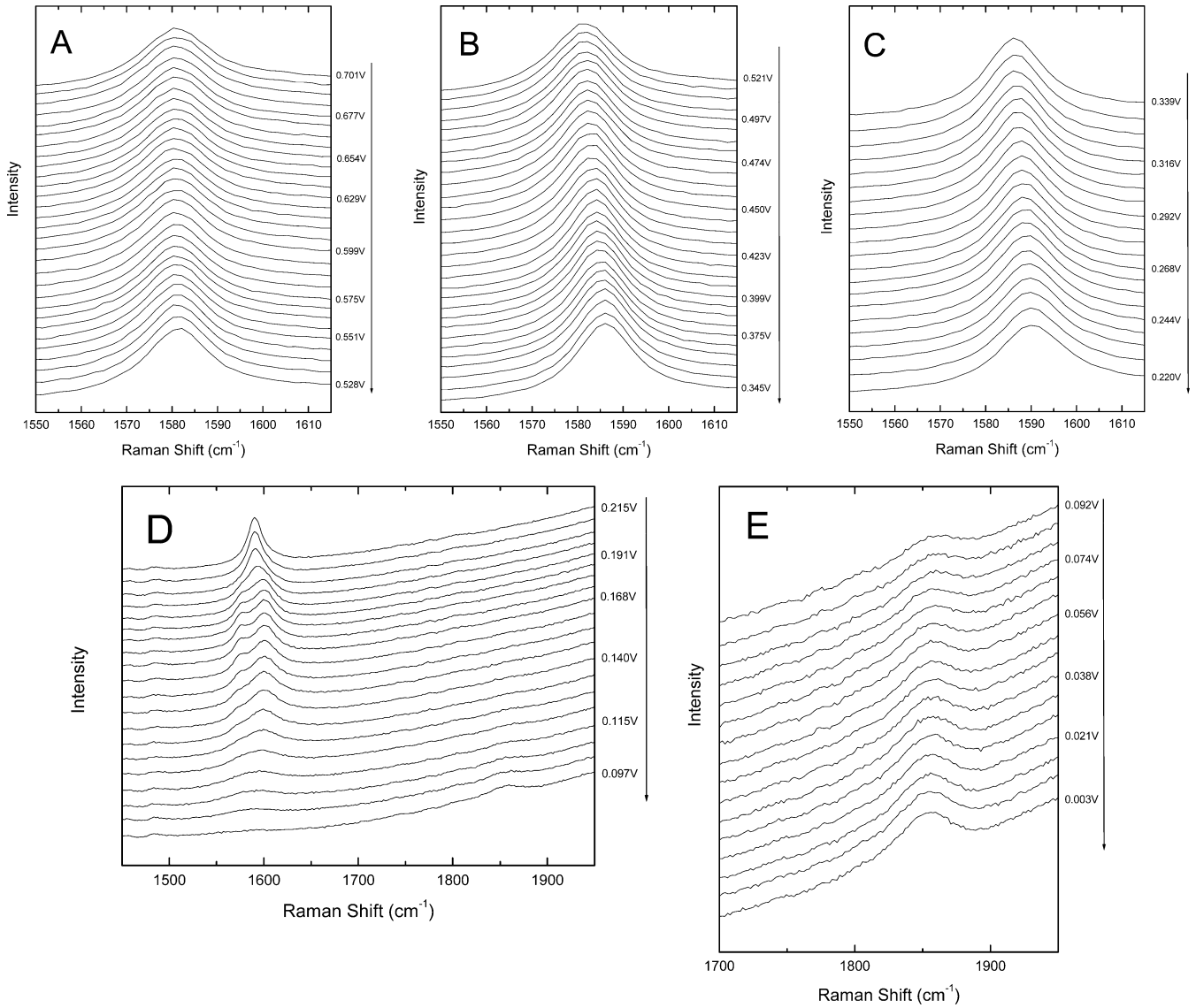

Figure 1. Series of in situ Raman spectra for a KS-44 graphite microflake recorded in 1 M $LiClO_4$ solution in a DEC/EC mixture (1:1 by volume), while acquiring the fourth linear voltammetric scan in the negative direction at a scan rate of 0.1 mV/s shown in Figure 2. The difference in average potential between two adjacent spectra is 6 mV. The arrows on the right-hand side of each panel indicate the direction of the scan.

Ar-filled glovebox, where the cell was filled with a 1 M $LiClO_4$ solution in a 1:1 (by volume) ethylene carbonate (EC):diethyl carbonate (DEC) mixture. A piece of Li metal foil (2 cm^2) pressed against a tungsten wire current collector was used as the counter/reference electrode. Once carefully sealed, the cell was removed from the glovebox for the spectroelectrochemical experiments.

The first linear potential scan of the graphite microflake was performed starting at 2.5 V in the negative direction down to ca. 0.0 V at a rate $\nu = 0.5$ mV/s, at which point the scan was reversed up to 0.7 V at the same scan rate. Two voltammetric cycles were then recorded in the range $0.7 > E > 0.0$ V at $\nu = 0.2$ mV/s. Once the potential returned to 0.7 V, ν was further reduced to 0.1 mV/s and a single linear scan performed down to 0.0 V while acquiring in situ Raman spectra continuously.

As described in detail elsewhere,[21] Raman spectra were recorded using a Raman 2000 system (Chromex Inc., Albuquerque, NM) incorporating a microscope attachment, using the 532 nm beam of a Verdi laser (Coherent) focused through a 10X Olympus microscope onto a KS-44 microflake (spot size of the beam was ca. 5 μm diameter) as the excitation source at powers on the sample of about 3 mW. The integration time for each frame was 15 s with four frames coadded to improve the signal-to-noise ratio. The electrode potential was controlled with a conventional potentiostat (AFRDE5, Pine Instruments), and all measurements were carried out at room temperature.

Statistical analysis of the spectra collected between 0.215 and 0.174 V was performed with the classical least squares under Matlab.

Results and Discussion

Shown in panels A through E in Figure 1 are a series of in situ Raman spectra recorded continuously for a KS-44 graphite microflake in 1 M $LiClO_4$ solution in a DEC/EC mixture (1:1 by volume) during the fourth linear voltammetric scan in the negative direction at a scan rate of 0.1 mV/s (see Figure 2). For clarity, the potentials at which the spectra in Figure 1 were collected have been specified for only a limited number of curves. Other values can, nevertheless, be calculated by assuming a 6 mV difference between adjacent spectra. Although subject to some error, owing to uncertainties in the actual shape of the background current (expected to have contributions due to processes other than simple Li^+ intercalation, such as

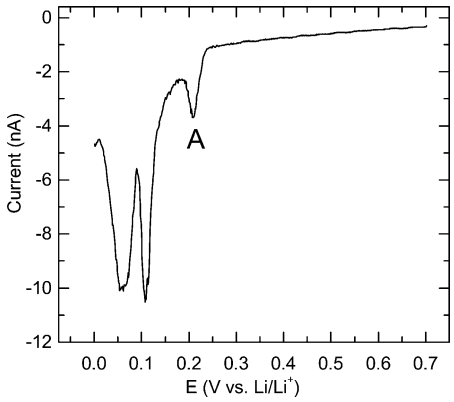

Figure 2. Fourth linear voltammetric scan recorded in the negative direction at a scan rate of 0.1 mV/s while acquiring the in situ Raman data in Figure 1.

electrochemically induced electrolyte decomposition), coulometric analysis of the voltammetric peak centered at about 0.21 V vs Li/Li$^+$, attributed to the dilute stage 1 → stage 4 phase transition[22]

$$LiC_{72} + Li^+ + e^- \rightarrow 2LiC_{36}$$

yielded a charge $Q = 0.55$ μC. On this basis, and given that the density of graphite is 2.25 g/cm^3, the weight of the microflake can be estimated to be of ca. 4.9 ng; hence, since the diameter of the fairly circular microflake is ca. 50 μm, i.e., cross-sectional area of 2×10^{-5}cm^2, its thickness would be of ca. 1 μm. Although reasonable, no attempts were made to measure this value by other means.

Close inspection of both the Raman and electrochemical data in these figures revealed excellent agreement with results reported by other groups using larger, more conventional electrodes,[13,14] providing strong evidence that the methods and procedures employed in this work are indeed highly reliable. In particular:

i. The Raman spectra of the KS-44 microflake down to ca. 0.22 V (see panels A−C) exhibit a single prominent peak at 1580 cm^{-1} ascribed (primarily) to the E_{2g2} mode of graphite. The asymmetric character of this peak is caused by the presence of a second feature centered at about 1604 cm^{-1} (X) attributed to electrochemically induced irreversible changes in the graphite induced by Li$^+$ intercalation into the lattice during the first scan in the negative direction. The relative contributions of the E_{2g2} and X features to the observed signal for spectra collected at four different potentials are shown in the Supporting Information (see Figure A, also item ii below).

ii. The peak position (PP) and full width at half-height (fwhh) of the E_{2g2} peak remained virtually constant in the potential range $0.7 > E > 0.58$ V vs Li/Li$^+$, i.e., no evidence for Li$^+$ intercalation into the graphite lattice; however, its integrated intensity, $I(E_{2g2})$, was found to increase by ca. 10% down to 0.5 V vs Li/Li$^+$ (see open circles in Figure B, Supporting Information). Also shown in that figure are the corresponding plots of I(X) as well as the total integrated intensity of the asymmetric feature $I(E_{2g2})$ and I(X) as a function of potential to illustrate the fact that the overall increase in integrated intensity is derived from $I(E_{2g2})$.

iii. As shown in Figure 3 (solid circles, right ordinate), fwhh-(E_{2g2}) decreased linearly in the range $0.4 < E < 0.6$ V, remained relatively constant down to 0.35 V, and then increased down to 0.25 V. In contrast, PP(E_{2g2}) increased linearly over the range 0.5−0.25 V vs Li/Li$^+$ at a rate of ca. −30 cm^{-1}/V (see solid line for which intercept = 1596.5 cm^{-1} and correlation coefficient = 0.9984), a behavior characteristic of dilute stage 1 (also known as phase VIII)[22] of the Li−graphite phase diagram.[23]

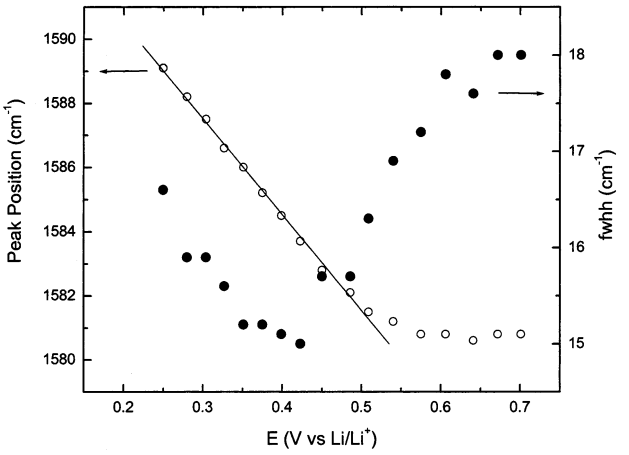

Figure 3. Plots of the peak position (open circles, left ordinate) and full width at half-height (fwhh, full circles, right ordinate) of the E_{2g2} mode extracted from a statistical analysis of spectra collected over the region 0.25−0.7 V. Within the region 0.5−0.25 V vs Li/Li$^+$, the E_{2g2} mode shifted linearly with potential (see solid line, slope = −28.9 cm^{-1}/V; correlation coefficient = 0.9924).

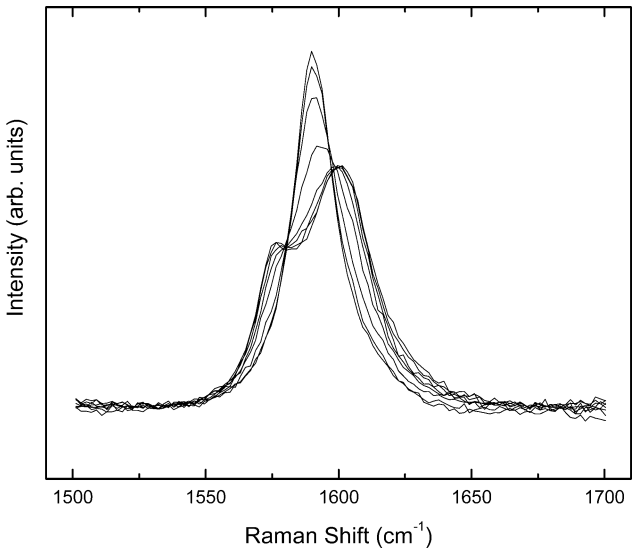

Figure 4. In situ Raman spectra in the potential region in which dilute stage 1 and stage 4 coexist, i.e., 0.215−0.174 V vs Li/Li$^+$ displayed in overlapping form to illustrate the presence of two clear isosbestic points at ca. 1580 and 1598 cm^{-1}.

iv. At potentials between 0.25 and 0.20 V, the E_{2g2} feature (see panel D, Figure 1) was found to gradually disappear, leading to the simultaneous emergence of two peaks centered at around 1601 and 1577 cm^{-1} (see below) attributed respectively to bounding and interior modes of stage 4 of the Li−graphite system.[13]

v. Within the range 0.170 down to 0.109, the interior mode of phase 4 decreased in intensity, rendering a spectrum displaying a single feature ascribed to phase 2.

vi. Further excursion into even more negative potentials led to the total disappearance of features in the spectral region about 1600 cm^{-1}; however, as clearly noted, a new peak (identified here for the first time) emerged at 1850 cm^{-1} (see panel E, Figure 1). Although this new feature cannot at this stage be assigned, data not shown in this work revealed that this latter

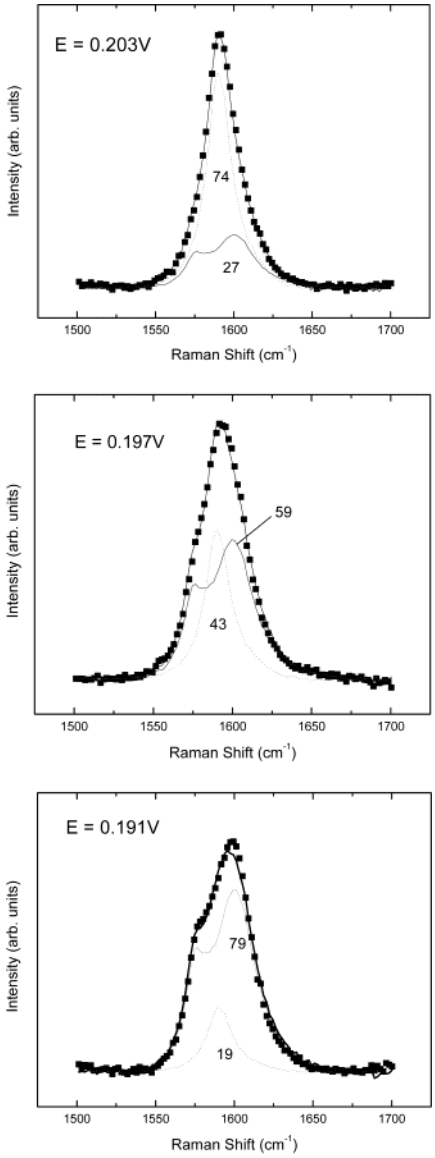

Figure 5. Three illustrative examples of the decomposition of spectral data in the potential region in which dilute stage 1 and stage 4 coexist. The scattered points are the experimental spectral data, and the thick solid line through them is the statistical fit in terms of contributions arising from dilute stage 1 (dotted line) and stage 4 (thin solid line). The spectra of the pure phases were obtained from data recorded at the two extremes of the potential range (see text for details). The numbers next of each of the curves represent the contribution of each phase to the experimental data as determined by statistical means (see text for details).

peak disappears upon scanning the potential positive, pointing to the reversible character of the process(es) responsible for its occurrence.

Although the development of procedures for the acquisition of in situ Raman spectra of a single graphite microflake, such as those implemented in this work, may be regarded in themselves as significant, the direct correspondence between the spectral features observed and the extent of Li^+ intercalation can offer new insights into thermodynamic and dynamic aspects of the Li/graphite system. In particular, strong evidence for a *quantitative* interconversion between dilute stage 1 and stage 4 was obtained from the presence of two clearly defined isosbestic points at 1598 and 1580 cm^{-1} for spectra collected in the range $0.174 \leq E \leq 0.215$ V, as shown in overlapping form in Figure 4. It becomes then possible to extract by statistical means (see

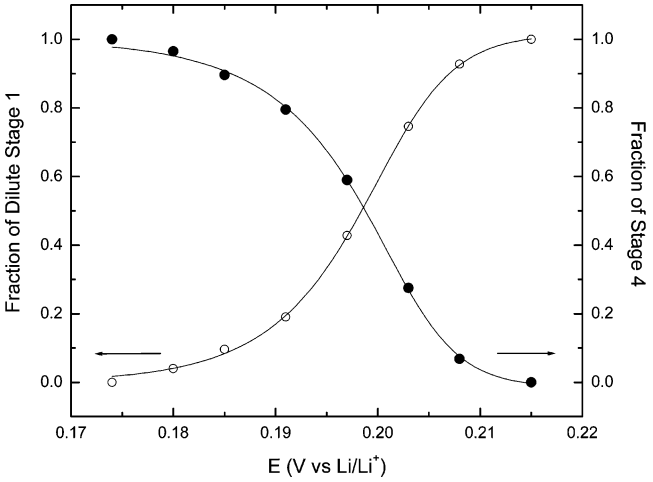

Figure 6. Plots of amount of the fraction of dilute stage 1 (left ordinate) and stage 4 (right ordinate) determined *independently* on the basis of statistical analysis of spectral data as shown in Figure 4. Dilute stage 1 and stage 4 phases are given by the spectra recorded at $E = 0.215$ and 0.174 V, respectively. The solid lines are best fits the data using arbitrary nonlinear functions.

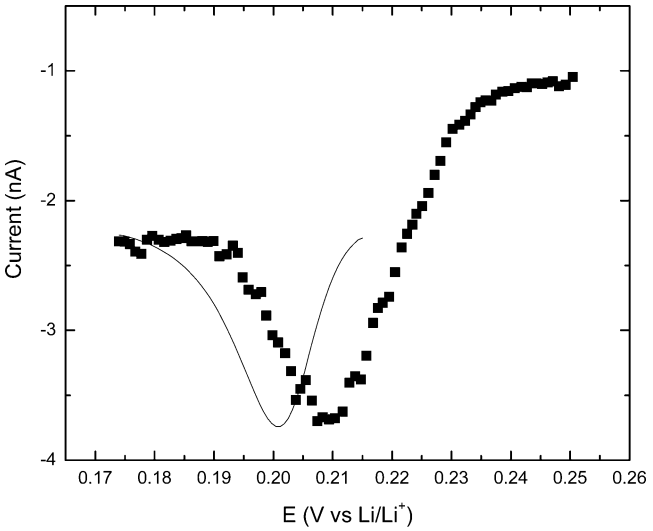

Figure 7. Expanded plot of the voltammetric data in Figure 2 in the range ca. $0.172 < E < 0.25$ V (scattered points) and normalized voltammetric peak (solid line) as deduced from the statistical analyses of the spectroscopic data in Figure 4 (see text for details).

Experimental Section) the amounts of each of the phases as a function of the applied potential, assuming the curves at $E = 0.215$ and 0.174 V represent the spectra of pure dilute stage 1 and pure stage 4, respectively. Three illustrative examples of such spectral decomposition are shown in Figure 5, where the scattered points are the experimental data, and the thick solid line through them is the statistical fit in terms of contributions arising from dilute stage 1 (dotted line) and stage 4 (thin solid line).

Plots of the fractions of dilute stage 1 (left ordinate) and stage 4 (right ordinate) determined independently on the basis of statistical analysis of spectral data shown in Figure 4 (and 5) are given in Figure 6. A similar tactic was employed recently for the quantitative analysis of the phase 1 ↔ phase 2 transition for $LiMn_2O_4$ based on in situ Raman data recorded for a single microparticle of the material.[20]

As has been pointed out in the literature, the dilute stage 1 → stage 4 transition corresponds to peak A in the linear scan given in Figure 2.[22] A direct correlation between spectral and

electrochemical data can be drawn by first fitting the experimental points to an arbitrary nonlinear function and then taking the derivative of the data in Figure 6. As shown in Figure 7, the results yielded two virtually overlapping peaks (only one is shown here) derived either from dilute stage 1 or *independently* from stage 4. Renormalization of the resulting feature to match the current maximum in peak A in the voltammogram yielded a value of fwhh almost identical to that found for the voltammetric peak. However, as clearly evident in Figure 7, the peak position extracted from the spectral data is about 10 mV more negative than that in the actual voltammogram. This slight shift is in all likelihood caused by a diffusional delay; i.e., the scan rate is still too fast compared to the time constant for mass transport of Li^+ within the graphite lattice. In other words equilibrium is only attained at a time longer and thus at a more negative potential than that prescribed under strict steady-state conditions. This diffusional lag could in principle be reduced by slowing down the scan rate; unfortunately, the much longer times required for a complete acquisition would make this approach highly impractical.

Summary

Quantitative analysis of in situ Raman spectra of a single KS-44 microflake electrode in a 1 M $LiClO_4$ solution in a 1:1 (by volume) ethylene carbonate (EC):diethyl carbonate (DEC) mixture made it possible to correlate features recorded over the potential region in which the dilute stage 1 to stage 4 transition of the Li/graphite system is known to occur, i.e., $0.174 \leq E \leq 0.215$ V vs Li/Li^+, with a prominent peak in the voltammogram of this material centered at ca. 0.21 V. This study provides yet another illustration of the power of Raman spectroscopy as a real time probe of intercalation phenomena in electrochemical environments. Efforts are currently under way to couple a computer-controlled X−Y translator to map in real time and with spatial resolution Li^+ insertion into the graphite lattice using a microflake electrode in the same configuration as that described in this work.

Supporting Information Available: Deconvolution of four representative Raman spectra for KS-44 microflake and plot of integrated peak intensity of the E_{2g2} and X modes as a function of potential. This material is available free of charge via the Internet at http://pubs.acs.org.

References and Notes

(1) Luo, Y.; Cai, W.-B.; Xing, X.-K.; Scherson, D. A. *Electrochem. Solid-State Lett.*, in press.
(2) Cai, W.-B.; Shi, Q.; Mansuetto, M. F.; Scherson, D. A. *Electrochem. Solid-State Lett.* **2000**, *3*, 319.
(3) Itoh, T.; Sato, H.; Nishina, T.; Matue, T.; Uchida, I. *J Power Sources* **1997**, *68*, 333.
(4) Kanoh, H.; Tang, W. P.; Ooi, K. *Electrochem. Solid-State Lett.* **1998**, *1*, 17.
(5) Totir, D. A.; Cahan, B. D.; Scherson, D. A. *Electrochim. Acta* **1999**, *45*, 161.
(6) Luo, Y.; Cai, W.-B.; Scherson, D. A. *Electrochem. Solid-State Lett.* **2001**, *4*, A101.
(7) Inaba, M.; Iriyama, Y.; Ogumi, Z.; Todzuka, Y.; Tasaka, A. *J. Raman Spectrosc.* **1997**, *28*, 613.
(8) Huang, W. W.; Frech, R. *J. Power Sources* **1999**, *82*, 616.
(9) Anzue, N.; Itoh, T.; Mohamedi, M.; Umeda, M.; Uchida, I. *Solid State Ionics* **2003**, *156*, 301.
(10) Dokko, K.; Mohamedi, M.; Anzue, N.; Itoh, T.; Uchida, I. *J. Mater. Chem.* **2002**, *12*, 3688.
(11) Totir, D. A.; Scherson, D. A. *Electrochem. Solid-State Lett.* **2000**, *3*, 263.
(12) Luo, Y.; Cai, W. B.; Scherson, D. A. *J. Electrochem. Soc.* **2002**, *149*, A1100.
(13) Inaba, M.; Yoshida, H.; Ogumi, Z.; Abe, T.; Mizutani, Y.; Asano, M. *J. Electrochem. Soc.* **1995**, *142*, 20.
(14) Huang, W.; Frech, R. *J. Electrochem. Soc.* **1998**, *145*, 3312.
(15) Totir, D. A.; Cahan, B. D.; Scherson, D. A. *Electrochim. Acta* **1999**, *45*, 161.
(16) Dokko, K.; Horikoshi, S.; Itoh, T.; Nishizawa, M.; Mohamedi, M.; Uchida, I. *J. Power Sources* **2000**, *90*, 109.
(17) Dokko, K.; Mohamedi, M.; Umeda, M.; Uchida, I. *J. Electrochem. Soc.* **2003**, *150*, A425.
(18) Dokko, K.; Nishizawa, M.; Mohamedi, M.; Umeda, M.; Uchida, I.; Akimoto, J.; Takahashi, Y.; Gotoh, Y.; Mizuta, S. *Electrochem. Solid-State Lett.* **2001**, *4*, A151.
(19) Uchida, I.; Mohamedi, M.; Dokko, K.; Nishizawa, M.; Itoh, T.; Umeda, M. *J. Power Sources* **2001**, *97*−*8*, 518.
(20) Dokko, K.; Shi, Q.; Stefan, I. C.; Scherson, D. A. *J. Phys. Chem. B* **2003**, *107*, 12549−12554.
(21) Luo, Y.; Cai, W.-B.; Scherson, D. A. *Electrochem. Solid-State Lett.* **2001**, *4*, A101.
(22) Levi, M. D.; Aurbach, D. *J. Electroanal. Chem.* **1997**, *421*, 79.
(23) Dahn, J. R. *Phys. Rev. B.* **1991**, *44*, 9170.